Performance of Terahertz quantum-well photodetectors

Jingyue Jia, and Yueheng Zhang

Key Laboratory of Artificial Structures and Quantum Control (Ministry of Education), Department of Physics and Astronomy, Shanghai Jiao Tong University, Shanghai 200240, China. jfxyqsh@163.com; yuehzhang@sjtu.edu.cn

***Abstract*—We investigated the performance of terahertz quantum-well photodetectors (THz QWPs) experimentally and theoretically. The photocurrent spectra of both THz QWPs are measured and simulated considering the many-particle effects. The dark current mechanisms are also investigated experimentally and theoretically. Results show that many-particle effects must be considered in the design of the THz QWPs. Also, the scattering assisted tunneling dark current should also be noted to play a very important role in the total dark current of THz QWPs.**

I. INTRODUCTION

Recently, considerable interest has been paid to THz quantum-well photodetector (QWP) which is a good candidate for compact terahertz systems originating from the characteristics of intersubband transition and unipolar transport. Compared with other detectors in THz region, such as Si bolometers, pyroelectric detectors and heterodyne detectors, THz QWPs have their own advantages [1]. The foremost important advantage relates to the availability of a mature material and processing technology for QWPs based on GaAs. Second, they are narrow band and enable wide wavelength coverage by adjusting the intersubband transition energy. The other advantage is their intrinsic high speed due to the inherent short carrier lifetime, which helps to create new applications. THz QWPs, as a natural extension of the traditional quantum-well infrared (IR) photodetector, have basically the same physical mechanism of detection and design rules. However, unlike IR QWP technology, THz QWP is far from mature and the performance needs substantial improvements since its first experimental demonstration [2]. First, additional physical effects, which in the IR region can be neglected, must be included. The low value of transition energy (small response frequency) of THz QWP necessitates the inclusion of many-particle effects, which adds extra computations and uncertainties. Second, the low barrier height results in larger dark current and low background-noise-limited performance (BLIP) temperatures, which seriously limits THz QWP's application scope [3]. We report two THz QWPs and discuss the photocurrent spectra and dark current mechanism in detail.

II. THEORY

Unlike QWPs in mid-infrared region, the quantum well of THz QWP is very shallow, therefore many-particle effects play a key role in band structures and the response peak frequency [4]. Within the effective mass approximation, the Schrodinger equation in the quantum well growth direction z is

$$\left\{-\frac{\hbar^2}{2}\frac{\partial}{\partial z}\left[\frac{1}{m^*(z)}\frac{\partial}{\partial z}\right]+V_{QW}(z)+V_H(z)+V_{xc}(z)\right\}\varphi_{l,kz}(z) = \varepsilon_{l,kz}\varphi_{l,kz}(z). \quad (1)$$

Here m^* is the electron effective mass, $\hbar$ is the reduced Planck constant, V_{QW} is the stepwise potential energy representing the conduction band offset profile, V_H is the Hartree potential energy obtained from Poisson's equation, V_{xc} is the exchange-correlation potential energy which is given by the local density approximation based on the density functional theory [5], $\varphi_{l,kz}$ is z-direction envelope function and $\varepsilon_{l,kz}$ is eigen-energy where l is miniband index and k_z is z-direction wavevector. Schrödinger equation and Poisson equation, along with exchange-correlation expression form a closed set which should be solved self-consistently. The self-consistency is realized by an iterative procedure until convergence is achieved [7]. In this paper, we numerically solve above equations using a plane-wave expansion method. In section III, we use the following criteria to check the convergence: $|(E_{F(i)}-E_{F(i-1)})/E_{F(i)}| \le 0.0001$, with $E_{F(i)}$ being the Fermi energy at the ith iterative step .

The calculation method of Fermi energy E_F is shown below. In the band structure of QWP, each eigen-energy $\varepsilon_{l,kz}$ corresponds to a subband or an in-plane parabolic band, i.e., the total energy of electron is $E = E_{kz} + \hbar^2 k_{||}^2/2m$, here $k_{||}$ is the in-plane wavevector in the x-y plane. The number of electrons on a given subband is $N_{l,kz}(E_F)$:

$$N_{l,k_z}(E_F) = \frac{m_{average}}{\pi\hbar^2} k_B T \ln\left[1+\exp\left(\frac{E_F-\varepsilon_{l,kz}}{k_B T}\right)\right] \quad (2)$$

where the average electron effective mass $m_{average}$ is defined as $m_{average} = m^*_w \int_{well} |\varphi_i(z)|^2 dz + m^*_b \int_{barrier} |\varphi_i(z)|^2 dz$, m^*_w (m^*_b) is effective mass in the well (barrier), k_B is the Boltzmann constant. Hence, the summation over all subbands equals the product of 2-dimensional (2D) doping density N_{2Ddope} and period number N_{QW} (the right-hand side of below equation):

$$\sum_{l,k_z} N_{l,k_z}(E_F) = N_{3Ddope} L_{dope} N_{QW} \quad (3)$$

Here, N_{3Ddope} is three-dimensional (3D) doping (usually with silicon for GaAs/AlGaAs materials system) concentration in a center region of quantum well (QW), L_{dope} is doping region width, $N_{2Ddope}=N_{3Ddope}L_{dope}$.

There physical processes contributes to dark current of THz QWPs. Firstly, interwell tunneling, which could be neglected due to the designed wide barriers, involves electrons scattering from the ground state in one quantum well (QW) into the next. Secondly, thermionic emission (TE) refers to thermal excitation of electrons from the upper part (with energy greater than the barrier height) of the ground state to the nonconfined continuum on the top of the barrier. Lastly, scattering-assisted Fowler-Nordheim tunneling (SAT) means confined electrons of the ground state slightly below the barrier height could be scattered by either phonons or electrons from QWs into the continuum through the tip of the barriers. L_w and L_b are the QW

width and barrier width, respectively. F is the electric field applied to the THz QWP samples. V_b is the original barrier height while $V = V_b - eFL_w/2$ is the barrier height lowering by applied electric field. According to the emission-capture model, we give the dark current by [6]

$$J_{dark} = \frac{ev(F)\tau_c}{\tau_{scatt}} \int_{E_1}^{\infty} \frac{m}{\pi\hbar^2 L_p} T(E,F) \left[1 + \exp\left(\frac{E - E_f}{k_B T}\right)\right]^{-1} dE \qquad (4)$$

The drift velocity is taken of the usual form $v(F) = \mu F/[1+(\mu F/v_{sat})^2]^{1/2}$. Values of μ = 5000 cm^2/Vs for the excited-electron mobility and $v_{sat} = 10^7$ cms^{-1} for the saturated velocity were used in calculation. τ_{scatt} is the scattering time of electrons from the ground state into the continuum state and τ_c is the capture time from the continuum back to the ground state. For sample L925 with transition energy ~47 meV, the life time of excited electron τ_c is mainly determined by optical phonon scattering and electron-electron scattering which is expected to have similar value as in mid-infrared QWPs. However, for L924 whose transition energy (28 meV) is smaller than the LO phonon energy of GaAs (36 meV), electron-electron scattering becomes the dominant mechanism, which is expected to cause a reduced capture probability and thus an increased τ_c. In this model, τ_c and τ_{scatt} just enter linearly and not in the exponent. As a result, a small deviation in the estimation of τ_c and τ_{scatt} will have weak impact on the results of dark current and BLIP temperature. So, the scattering time is set as τ_{scatt} = 5 *ps*, the values of life time of excited electrons are set as τ_c = 8 *ps* for sample L925 and τ_c = 10 *ps* for L924. L_p is the period length of the multiple quantum-well structure and equals the sum of QW and barrier widths. $T(E,F)$ is the transmission coefficient calculated using Wentzel-Kramers-Brillouin (WKB) approximation. For energy higher than the barrier (for $E > V$), $T(E,F) = 1$. Eq. (4) could be simplified in pure TE regime and the dark current obtained corresponds to TE dark current as marked in Fig. 1. For energy less than the barrier height, $T(E,F)$ could be given as:

$$T(E,F) = \exp\left[-2\int_0^{z_c} dz\sqrt{2m_b(V - E - eFz)}/\hbar\right], \qquad (5)$$

where m_b is the barrier mass, $z_c = (V-E)/eF$ is defined as the classical tunneling point. As shown in Fig. 1, when $V-eFL_b < E < V$, the dark current obtained corresponds to SAT dark current. When $E_1 < E < V-eFL_b$, the dark current obtained corresponds to interwell tunneling dark current which is far less than TE and SAT dark current in operation temperatures and biases.

III. Discussion

TABLE I. SAMPLE DETAILS

Sample	L_w (nm)	L_b (nm)	Al_x (%)	N_{3Ddope} (cm^{-3})	L_{dope} (nm)	N	ν_p (THz)
L924	12	64	4	1×10^{17}	7	35	6.78
L925	9.6	50	7	1×10^{17}	9.6	40	~ 11.37

The black lines in Fig. 1 are the measured photocurrent spectra in 12 K for both samples. The main dark region from 256 to 292 cm^{-1} in sample L924 is due to GaAs optical phonon absorption in the substrate, other small features such as the dips at 312 and 338 cm^{-1} are caused by two-phonon absorption. The dip at 362 cm^{-1} in both samples corresponds to the AlAs-like phonon absorption. The dotted and dash-dotted lines are spectra without and within many-particle effects, which indicated that many-particle effects must be included.

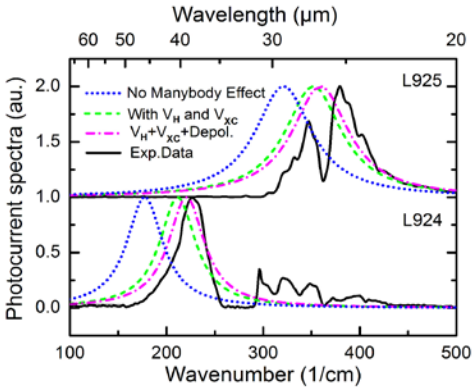

Fig. 1 Measured and Calculated photocurrent Spectra

Fig. 2 is the measured and calculated dark current for both samples. It is clear that, unlike previous study, scattering assisted tunneling (SAT) dark current are also very important for the total dark current for THz QWPs as well as thermal emission (TE) regime. Especially in the high bias region, SAT dark current can be much larger (i.e., nearly ten times) than the TE dark current.

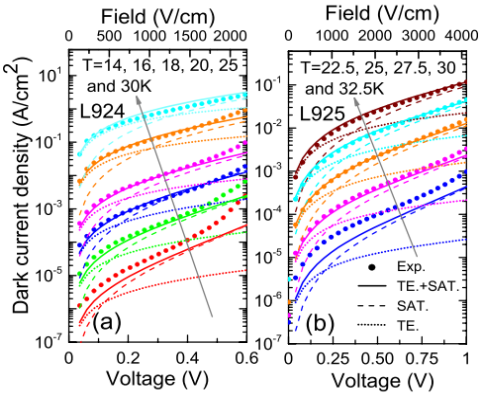

Fig. 2 Measured and Calculated Dark current

References

[1]. X. G. Guo, J. C. Cao, R. Zhang, Z. Y. Tan, and H. C. Liu, "Recent Progress in Terahertz Quantum-Well Photodetectors," *IEEE J. Sel. Top. Quantum Electron.*,vol. 19, no. 1, pp. 8500508, Feb. 2013.

[2]. H. Luo, H. C. Liu, C. Y. Song, and Z. R. Wasilewski, "Background-limited terahertz quantum-well photodetector," *Appl. Phys. Lett.*, vol. 86, pp. 231103, Jun. 2005.

[3]. J. Y. Jia, J. H. Gao, M. R. Hao, T. M. Wang, W. Z. Shen, Y. H. Zhang, *et al.*, "Dark current mechanism of terahertz quantum-well photodetectors, " *J. Appl. Phys.*, vol. 116, pp. 154501, Oct. 2014.

[4]. S. Zhang, T. M. Wang, M. R. Hao, Y. Yang, Y. H. Zhang, W. Z. Shen, *et al.*, "Terahertz quantum-well photodetectors: Design, performance, and improvements, " *J. Appl. Phys.*, vol. 114, pp. 194507, Nov. 2013

[5]. J. Zhang, and W. Pötz, "Exchange-correlation effects in resonant-tunneling heterostructure," *Phys. Rev. B.*, vol. 42, no. 17, pp. 11366-11369, Dec. 1990.

[6]. H. Schneider and H. C. Liu , "Quantum Well Infrared Photodetec-tors—Physics and Applications," . Berlin, Germany: Springer-Verlag, 2007, vol. 126, Springer Series in Optical Sciences.